Inviscid Theory of Wall Interference in Slotted Test Sections

Sune B. Berndt*
The Aeronautical Research Institute of Sweden (FFA), Bromma, Sweden

The classical theory of longitudinally slotted walls, which substitutes an approximate homogeneous wall boundary condition for the true mixed conditions, is extended in several respects. Based on recent experimental findings at the FFA, an inviscid flow model is adopted in which the outgoing slot flow penetrates into the plenum chamber as a thin jet, while the re-entering flow, admitting quiescent air from the plenum chamber into the test section, induces a longitudinal separation bubble at plenum pressure along the slot and adjacent parts of the test section wall. The three-dimensional analysis, based on the assumption that the slots are narrow, retains quadratic cross-flow terms in the pressure equation and allows the slots to be few in number and have nonuniform distribution and geometry. A family of homogeneous boundary conditions is obtained, each of successively higher accuracy. Application to the design of interference-free transonic test sections is discussed. Unsteady effects also are considered.

Nomenclature

$a(x)$	= slot width; Fig. 5
d	= arc length between slots; Eq. (29)
$E(y)$	= unit step function
$\mathfrak{F},\mathfrak{F}^{-1}$	= functionals on S_w; Eq. (26)
Grad, $\underline{\Delta}$	= differential operators in plane x = const
$H^{(i,k)}$	= Eq. (18)
$K(x)$	= coefficient in slotted-wall boundary condition; Eqs. (32, A8, and A12)
M	= Mach number of reference flow
M_o	= entrance Mach number; Fig. 2
N	= number of slots
p	= pressure
$p_p^{(i)}$	= pressure in plenum chamber i
p_∞	= pressure of flow at Mach number M
$Q(z,y)$	= normalized slot flow potential; Eq. (19)
$q^{(i)}(x,t)$	= flux (per unit length) through slot i; Sec. VI.
r	= radius vector in cross-flow plane
r,θ	= polar coordinates in cross-flow plane
$r^{(i)}$	= distance from slot point i; Fig. 4, Eq. (11)
$r^{(i,k)}$	= distance between slot points i and k; Eq. (18)
S_m	= cylindrical surface enclosing the model and its wake; Fig. 2
S_p	= free surface between fast air and quiescent plenum air; Fig. 1
S_{po}	= surface at plenum pressure across jet on plenum side of slot; Fig. 1
S_w	= outer boundary of test section; Fig. 2
t	= time
U	= flow velocity at Mach number M
$v(y)$	= $\partial Q/\partial y$ on $z=0$; Eq. (23)
x	= distance along tunnel axis; Fig. 2
x_o	= location of entrance section; Fig. 2
y,z	= Cartesian coordinates at slot; Fig. 5
y_p	= coordinate of S_p on slot center-line; y_{po} corresponds to S_{po}; Fig. 5
γ	= ratio of specific heats
$\delta^{(i)}$	= nondimensional plenum pressure difference; Eq. (5)
$\varphi,\bar{\varphi}$	= perturbation velocity potentials; Eqs. (1) and (6)
$\phi,\bar{\phi}$	= harmonic functions in cross-flow plane; Eq. (7)
ν	= highest order considered in harmonic analysis of interference; Eq. (8)
ρ_∞	= density of flow at Mach number M

Received Oct. 13, 1976.
Index categories: Computational Methods; Transonic Flow; Research Facilities and Instrumentation.

*Consultant; also Professor of Gasdynamics, Royal Institute of Technology, Stockholm, Sweden. Member AIAA.

I. Introduction

IT is a remarkable fact that theory plays a very minor roll in the design and use of slotted transonic test sections; in particular, when one considers that the theory was already well-developed at an early stage.[1-3] There might be several reasons for this, but one seems to be that the flow models, mainly inviscid ones, had not been verified at the time by experiments, while inconsistencies were alleged to appear in trying to apply the theoretical results directly to practical wind-tunnel flows. Therefore, it seems, reliance was placed on empirical methods, determining the slot width so as to minimize choking effects around Mach one, and accepting as freestream conditions the upstream conditions in the empty test section as calibrated against the plenum pressure. It became a widespread belief that viscous effects of an unknown and complicated nature are present in the slot flow, and that therefore an empirical approach is all that is available. In consequence, the development of the theory came to a virtual standstill.

In a recent experimental investigation of slot flows[4] it has been found that under typical test conditions the slot flow is not necessarily dominated by viscosity, and that therefore one can define an inviscid flow model that is reasonably close to reality. This model, which is not as simple as some of the early ones, will be set down in the next section. For a fuller discussion of the problems involved, see Ref. 4 and references given therein.

Our present task is to base a general inviscid theory on this model for the wall interference caused by a slotted wall. In the classical theory of this kind,[5-8] based on the slender-body approximation, a description is obtained of the combined effect of the mixed boundary conditions at the slots and slats in the form of a far simpler, homogeneous boundary condition, relating the average pressure difference across the wall to the average streamline curvature normal to the wall. The

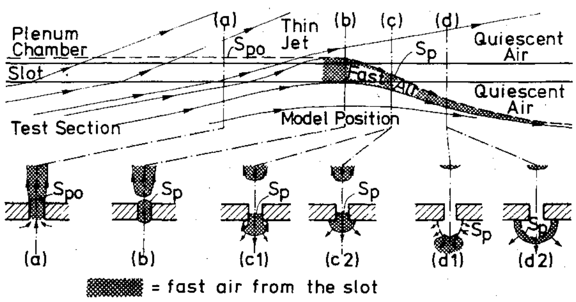

Fig. 1 Possible inviscid flow patterns (not to scale).

simplification is made possible by postulating a large number of simlar slots uniformly distributed over the interfering wall.

In order to minimize any viscous effects, and possibly for other reasons, it is desirable to keep the number of slots small. Furthermore, if the slots are few in number, their proper location might become important when minimizing the wall interference. Consequently, there is a great need for freeing the classical theory from its inherent restrictions while keeping its simplicity. We shall achieve this by employing a modified method of approximation, based on the much less restrictive assumption that the slot width is small as compared to the distance between slots. From the case of uniform slot distribution, this is known to be a workable approach.[9,10] In the present more general context, it leads to a straightforward application of the method of matched asymptotic expansions.

In our analysis we shall aim at a fair level of generality. This might, for example, facilitate later inclusion of corrections for viscous effects. The main concern will be with three-dimensional tests, the case of two-dimensional tests having already been treated.[4] Also, we shall not exclude the case of unsteady flow, which is clearly quite important in connection with oscillatory testing.[11] However, in the present paper, the applications of the theory will be restricted to a few very simple cases.

The theory turns out to produce not one, but a whole family of possible homogeneous boundary conditions, each corresponding to a specific degree of resolution of the details of the wall flow as filtered through the averaging procedure. The choice for any particular application will have to be based on considerations of accuracy. There also is some freedom in the method of applying the boundary conditions, depending on the kind of problem to be solved. If the slots are to be adjusted for zero interference by employing measured wall pressure distributions,[5,12] a somewhat different type of boundary condition will be required than if the adjustment is to be based on a precomputed interference-free flowfield. We shall return to this point in later sections, as well as to the related questions of how to define and compute wall interference corrections and how to use test section calibrations.

II. An Inviscid Model for the Slot Flow

The slot flow model to be adopted is presented in Fig. 1. In the upstream part of the test section, the flow is going outward through the slot into the plenum chamber, where it forms a thin jet. The flow inside the slot is attached, as indicated in cross section *a*, and separation occurs at the sharp slot edges on the plenum side. Above the model, the slot flow turns back, leaving the jet to continue on its own into the interior of the plenum chamber. This splitting of the fast air into two separate streams is shown, beginning at section *b*. At *c*, the fast air in the slot, having entered farther upstream, is returning to the test section. At *d*, the fast air has left the slot, and behind it appears a bubble of quiescent air at plenum pressure, the boundary of which is expanding into the test section flow. Typically, the bubble is narrow and extends along the slot. Presumably it collapses onto the slot farther downstream if the cross-flow turns back again toward the wall. What happens if it is struck by a shock-wave from the model is not known.

This is the picture of the slot flow found in Ref. 4. The description leaves undecided whether the fast air returning from the slot to the test section is a vorticity-carrying slug, as in *c1* and *d1*, or whether it expands around the slot edges without separation, as in *c2* and *d2*. The experimental evidence,[4] although not quite conclusive, points to the former alternative. It might well be that both types of flow may occur. In order to avoid complications at this stage we shall assume the second type of flow, but when developing the analysis we shall keep the alternative in mind, as well as the possible need for viscous corrections.

In order to translate the slot flow model into a set of boundary conditions to be used with the flow equations, further simplifications must be introduced. First of all, there is no need to consider in detail the development of the jet inside the plenum chamber. From the point of view of the slot flow, it should be sufficient to designate a surface S_{po} across the slot exit on which the plenum pressure may be taken to act. It also must be specified how the fast air in the slot is split off to return to the test section: making the obvious choice, we shall assume that the downstream end of S_{po} coincides with the upstream end of the free surface S_p, which is the boundary between the fast air and the quiescent plenum air (see Fig. 1). Thus, S_{po} and S_p together form a surface on which we have plenum pressure. Obviously there is no need, nor any real possibility, to determine S_{po}, and hence S_p in its subsequent development, with any accuracy. We shall interpret this as a license to make a choice that renders the analysis simple.

Having so far tacitly assumed that the flow is steady, we must also consider how the flow model can be generalized to become applicable to unsteady flows. Obviously, the free surface S_p must be allowed to move. The possibility that pressure waves propagate inside the plenum chamber also must be considered. Consequently, the pressure on $S_{po}+S_p$ cannot be taken to be known in advance. These are serious complications, which perhaps cannot be handled without making further simplifications, such as assuming the unsteadiness to be a small perturbation of a steady flow.

III. Assumptions and Basic Equations

The test section wall, before the slots are introduced, is taken to be a cylinder S_w (Fig. 2). The longitudinal slots, numbered 1 to N, are connected to plenum chambers with quiescent air at prescribed pressures $p_p^{(i)}$ $(i=1,2,\ldots,N)$. The x axis, parallel to S_w, points in the flow direction. The radius vector r is orthogonal to the x axis. The hydraulic radius of S_w is employed as the unit of length.

The model and its wake are located within the cylinder S_m, parallel to S_w. The flow is taken to be inviscid between S_m and S_w, as well as in the slots and plenum chambers. The flow of fast air will be described by a small irrotational perturbation of a uniform reference flow parallel to the x axis (at density ρ_∞, pressure p_∞, velocity U and Mach number M); the perturbation is considered to be produced by the distribution of normal velocity set up by the model on S_m. This distribution is, of course, not known in advance. Our ignorance of the flow inside S_m is the reason for the wind-tunnel test, but from the shape of the model one often can estimate it with sufficient accuracy for computing the wall interference. This we assume to be so, and so choose for the reference state the freestream state at which the estimate is made.

Let $U\cdot\varphi(x,r,t)$ be the perturbation velocity potential, normalized to be zero in the reference flow. To the first order, for transonic flow, it satisfies the following differential equation between S_m and the outer boundary of the fast air:

$$\underline{\Delta}\varphi=[M^2-1+M^2(\gamma+1)\varphi_x]\varphi_{xx}+\frac{2M^2}{U}\varphi_{xt}+\frac{M^2}{U^2}\varphi_{tt} \tag{1}$$

Here $\underline{\Delta}$ is the Laplacian in planes $x=\text{const}$ whereas γ is the ratio of specific heats in the reference state. The inner boundary condition for φ is at a point P on

$$S_m\ :\ \varphi_n=F(P,t) \tag{2}$$

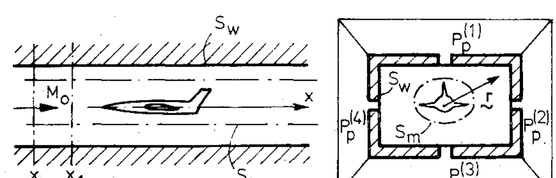

Fig. 2 Slotted test section.

where n denotes differentiation in the normal direction and F is the normal velocity distribution (which we have assumed known). The outer boundary condition on solid surfaces adjacent to fast air is similar: on

$$S_w \text{ between slots: } \varphi_n = 0, \text{ internally in slots: } \varphi_n = H(P) \quad (3)$$

H vanishes wherever the walls of the slots are parallel. More generally, we easily could allow φ_n to be nonvanishing on S_w as well, thus accounting for small deviations from cylindrical geometry, as well as for the displacement effect of wall boundary layers. Contouring the slats might be a useful method for helping the slots do a good job.[12,13]

The remaining outer boundary condition involves the pressure. In the present approximation, the Bernoulli equation is

$$p - p_\infty = -\rho_\infty U^2[(1/U)\varphi_t + \varphi_x + \tfrac{1}{2}\mathrm{Grad}^2\varphi] \quad (4)$$

where "Grad" denotes the gradient operator in a plane x=const. The quadratic cross-flow term is needed only in the slot regions, where the cross-flow velocity might be considerably larger than elsewhere. In the case of steady flow, the jet and free-surface boundary condition therefore takes the form on

$$S_{po} + S_p \ : \ \varphi_x + \tfrac{1}{2}\mathrm{Grad}^2\varphi = -\delta^{(i)}$$

$$\delta^{(-i)} \equiv (p_p^{(i)} - p_\infty)/\rho_\infty U^2 \ (i = 1, \ldots, N) \quad (5)$$

The corresponding condition for unsteady flow will be discussed later.

In order to formulate an upstream boundary condition, we shall assume that the slots all begin at $x = x_o$, and that their widths increase smoothly from zero. With a stretch of parallel walls between the contraction and the beginning of the slots—since F is likely to be small that far upstream—the flow at $x = x_o$ ought to be uniform (except for receding waves in the unsteady case). We shall in fact take this to be so, and prescribe as an upstream boundary condition for steady flow that φ takes a constant value, φ_o say, on the plane $x = x_o$. At the same time we must adjust F in a region $x_o \leq x < x_1$, say, in order for it to vanish smoothly at x_o (Fig. 2). Note that the Mach number M_o of the entrance flow is a controllable test parameter, which determines a particular value for φ_x. We shall not specify any downstream boundary condition; only assume that the slotted part of the test section is long enough for the conditions at the downstream end not to influence the flow at the model.

In the present approach, the wall interference is obtained, obviously, by subtracting from φ on S_m the corresponding distribution obtained with unbounded flow outside S_m (using the same reference flow) in precisely the situation prescribed when estimating F. If we are to minimize the interference, we must explore the influence on φ of the several test parameters at our disposal. The mixed form of the set of outer boundary conditions for φ constitutes a major difficulty when performing this task.

IV. Method of Approximation

In order to overcome this obstacle, we shall introduce an approximation $\bar{\varphi}(x,r,t)$ for φ, satisfying the same differential equation and the same inner boundary condition, but a new outer boundary condition. This boundary condition ought to be as simple as possible from the point of view of computing $\bar{\varphi}$, consistent with the requirement that $\bar{\varphi}$ must be nearly equal to φ on S_m (where the interference is to be computed). Thus, the new boundary condition shall be required to be homogeneous and local in the sense that it is a regular functional relationship betwen $\bar{\varphi}$ and its normal derivative over the entire boundary S_w, whereas values of $\bar{\varphi}$ or $\bar{\varphi}_n$ inside S_w, e.g. on S_m, must not be explicitly present. Clearly, the boundary conditions for φ are not homogeneous in this sense, although they are local.

The potentials $\bar{\varphi}$ and φ are expected to be nearly equal almost everywhere, in particular in the neighborhood of S_m, and to be essentially different only where slots are located. There the cross-flow derivatives, but not the potentials themselves or their derivatives with respect to x or t, are expected to be much different. Noting that the differential equation (1) contains cross-flow derivatives only in the left-hand member, we arrive at our basic method of approximation: we neglect the difference between $\bar{\varphi}$ and φ in the right-hand member, and postulate that

$$\underline{\Delta}(\bar{\varphi} - \varphi) = 0 \quad (6)$$

This is of course the slender-body approximation applied to the slot flow. There is additional support for its validity in that, in transonic flow, and at low frequencies, all terms in the right-hand member of Eq. (1) are small. But this also points to the danger that the approximation in Eq. (6) may not be very good near shock waves and high-frequency receding waves. At best, the approximation can be verified a posteriori.

The differential equation (6) can be integrated immediately to give

$$\varphi = \bar{\varphi} + \phi - \bar{\phi} \quad (7)$$

where $\phi(r;x,t)$ and $\bar{\phi}(r;x,t)$ are two-dimensional harmonic functions satisfying the same type of boundary condition as φ and $\bar{\varphi}$. More specifically, ϕ is taken to satisfy an inner condition (2) with the normal derivative prescribed as $f(P,t)$ on S_m (f being similar to, but in general different from F); in addition, it must satisfy the condition (3) for the normal derivative at the outer boundary, as well as the conditions (5) for the slot pressures (or a corresponding set for unsteady flow). In general, this will determine ϕ uniquely in terms of f. Similarly, $\bar{\phi}$ is taken to satisfy the same inner boundary condition for the normal derivative as ϕ, and a new homogeneous and local outer boundary condition chosen to make $\bar{\phi}$ uniquely determined and easy to calculate, rendering it at the same time nearly equal to ϕ on S_m.

If the outer boundary condition for $\bar{\phi}$ has the required property of not containing f explicitly, then it might be eligible as the condition defining $\bar{\varphi}$. Let us assume this to be so, and solve Eq. (1) for $\bar{\varphi}$, applying the inner boundary condition (2) together with the outer boundary condition thus taken over from $\bar{\phi}$. This can be done without specifying f. We then conclude from Eq. (7), assuming the basic approximation (6) to be true, that $\bar{\varphi}$ is nearly equal to φ on S_m, as it should be.

The crucial question is now whether φ, as approximated by Eq. (7), satisfies the outer boundary conditions (3) and (5) to sufficient accuracy. To verify this, choose f so as to make $\bar{\phi}_n = \bar{\varphi}_n$ on S_w. The equality of $\bar{\phi}$ and $\bar{\varphi}$ on S_w (in virtue of the common boundary condition) is thereby extended, approximately, to a neighborhood of S_w. Therefore, in consequence of (7), it might be assumed that in a similar neighborhood (which is taken to include the slots) $\varphi \simeq \phi$, $\varphi_x \simeq \phi_x$, $\varphi_t \simeq \phi_t$, Grad $\varphi \simeq$ Grad ϕ, and also that the free boundaries S_p coincide. Then φ satisfies the boundary conditions (3) and (5), and the problem of computing φ on S_m, as influenced by the test section wall, has been reduced to the simpler problem of computing $\bar{\varphi}$.

Note that in this process it might be unnecessary to compute ϕ, f, or $\bar{\phi}$, since none of them is present in the boundary condition for $\bar{\varphi}$. However, if we want to determine conditions at the wall, for example wall pressures, then we shall need to know ϕ there.

V. Conformal Mapping and Analytic Continuation: Smoothing

In order to arrive at the outer boundary condition for $\bar{\varphi}$ we must analyze ϕ and $\bar{\phi}$. They are both two-dimensional harmonic functions in regions with shapes independent of x. It is therefore natural to perform a conformal mapping of the annular region between S_w and S_m in each plane $x=$const, mapping the boundaries onto concentric circles. In addition to other simplifications, this will permit us to reformulate the inner boundary conditions for ϕ and $\bar{\phi}$ by analytic continuation to be imposed at the center of the circles.

The mapping is scaled to leave the cross-sectional area of S_w invariant. Let (r,θ) be polar coordinates in the transformed plane. Hence, S_w is mapped onto the unit circle. We now postulate that, in analyzing $\bar{\phi}(r,\theta;x,t)$, it is sufficient to include only terms up to and including the order ν in a Fourier expansion with respect to θ. This is a decisive step: it specifies a filter, which permits us, by choice of ν, to approximate ϕ by $\bar{\phi}$ with controllable smoothness at the wall and precision at the model. Then $\bar{\phi}$ must have the form

$$\bar{\phi}=A_o \ln r+\bar{D}_o+\sum_{j=1}^{\nu}[(A_j\cos j\theta+B_j\sin j\theta)r^{-j}+(\bar{D}_j\cos j\theta+\bar{E}_j\sin j\theta)r^j] \qquad (8)$$

where the coefficients A_o, A_j, B_j, $\bar{D}_j$, and $\bar{E}_j$ all are functions of x and t.

The corresponding expression for $\phi(r,\theta;x,t)$, having the same singular structure at the origin, is

$$\phi=A_o \ln r+D_o+\sum_{j=1}^{\nu}[(A_j\cos j\theta+B_j\sin j\theta)r^{-j}+(D_j\cos j\theta+E_j\sin j\theta)r^j]+\delta \qquad (9)$$

where the remainder δ, containing the harmonic components required for describing details of the slot flow, is $O(r^{\nu+1})$ as $r\rightarrow 0$. In this formulation, the requirement of common singular structure corresponds to the condition that the $\bar{\phi}$ and ϕ have the same normal velocity on S_m, whereas the requirement that the outer boundary condition for $\bar{\phi}$ makes it nearly equal to ϕ on S_m now takes the form

$$\bar{D}_o=D_o \ , \ \bar{D}_j=D_j, \ \bar{E}_j=E_j \qquad (j=1,2,...,\nu) \qquad (10)$$

Once the outer boundary condition has been established, we can either use it directly to solve the complicated transformed version of the transonic differential equation, or transform it back to the original geometry and there apply it to the simpler original equation. The choice is one of convenience in the numerical work. In the following, we shall be concerned only with establishing the outer boundary condition in the circular geometry.

VI. Asymptotic Approximation for Narrow Slots

The fact that, in practice, slots are usually narrow as compared to distances between slots will be the basis for the continued analysis. In this situation, asymptotic expansion with respect to the slot width as a small parameter suggests itself as a useful method to be adopted. Obviously, each slot will need its own "inner" expansion, scaled with the slot width. The "outer" expansion will be concerned with the overall flow on the scale of the test section radius.

In an inner expansion the slot will be located alone in an infinite plane wall (Fig. 3). In the outer expansion, the test section wall will be solid with sinks or sources located at the points into which the slots have contracted. The total flux of each sink or source will of course be equal to twice the corresponding flux $q^{(-i)}$ $(i=1,2,...,N)$ through the slot (positive if into the plenum chamber; flux unit $=U$ times test section radius). These fluxes are not known in advance, but depend on the plenum pressures $p_p^{(i)}$ through the pressure conditions (5) at the boundaries S_{po} and S_p. Therefore, they will have to be obtained by matching the outer expansion to each of the inner expansions. For a survey of matching problems involving flow through narrow slots, see Ref. 14.

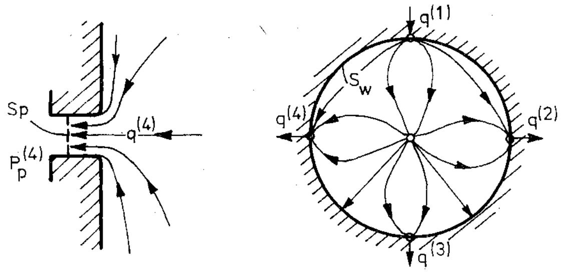

Fig. 3 Inner and outer flows.

Leaving the inner expansions for later, we shall first obtain an outer representation of ϕ, assuming the fluxes $q^{(i)}$ to be known. This will permit us to analyze $\bar{\phi}$ and, in fact, to make a first specification of the boundary condition for $\bar{\phi}$.

An elementary solution with a source at the origin and a sink of double strength on the unit circle at $\theta=\theta^{(i)}$ (Fig. 4) is given by $(1/2\pi)\ln r-(1/\pi)\ln r^{(i)}$, where $r^{(i)}(r,\theta)$ is the distance from the sink:

$$r^{(i)}=\sqrt{1-2r\cos(\theta-\theta^{(i)})+r^2} \qquad (11)$$

It is shown easily that this solution has zero normal derivative on the unit circle (for $\theta\neq\theta^{(i)}$). Therefore we can write down the outer representation of ϕ immediately:

$$\phi=\frac{1}{2\pi}\left(\sum_{i=1}^{N}q^{(i)}\right)\ln r-\frac{1}{\pi}\sum_{i=1}^{N}q^{(i)}\ln r^{(i)}+G(r,\theta) \qquad (12)$$

The undetermined function G is harmonic in the unit disk, except at the origin, and has zero normal derivative at the outer boundary. Comparison with Eq. (9) shows that $A_o=\Sigma q^{(i)}/2\pi$ and that

$$G=D_o+\sum_{j=1}^{\nu}(A_j\cos j\theta+B_j\sin j\theta)(r^{-j}+r^j) \qquad (13)$$

In order to obtain $\bar{\phi}$ we must expand the rest of ϕ. It is easy to show that

$$\ln r^{(i)}=-\sum_{j=1}^{\nu}\frac{1}{j}\cos[j(\theta-\theta^{(i)})]r^j+O(r^{\nu+1}) \qquad (14)$$

Hence,

$$\bar{\phi}=\frac{1}{2\pi}\left(\sum_i q^{(i)}\right)\cdot\ln r+D_o+\frac{1}{\pi}\sum_i q^{(i)}\left\{\sum_j\frac{1}{j}\cos[j(\theta-\theta^{(i)})]r^j\right\}+\sum_{j=1}^{\nu}(A_j\cos j\theta+B_j\sin j\theta)(r^{-j}+r^j)$$

$$=\phi+\frac{1}{\pi}\sum_{i=1}^{N}q^{(i)}\left\{\ln r^{(i)}+\sum_{j=1}^{\nu}\frac{1}{j}\cos[j(\theta-\theta^{(i)})]r^j\right\} \qquad (15)$$

This immediately gives an important part of the attempted outer boundary condition for $\bar{\phi}$:

$$r=1: \ \bar{\phi}_r=\frac{1}{\pi}\sum_{i=1}^{N}q^{(i)}\left\{\frac{1}{2}+\sum_{j=1}^{\nu}\cos[j(\theta-\theta^{(i)})]\right\} \qquad (16)$$

This expression for the normal derivative of $\bar{\phi}$ at the outer boundary does not contain the coefficients A_j and B_j explicitly (these coefficients represent the shape of the model),

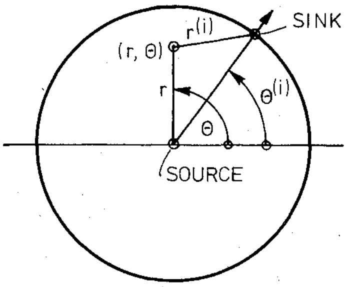

Fig. 4 A source at the origin, a sink of double strength on the unit circle.

and so it seems to be local as well as homogeneous in the previously defined sense. One might suspect that the unknown fluxes $q^{(i)}$, when resolved, will bring the model back into the picture, but since they are to be obtained by matching at the slots, we expect them, of course, to be determined locally in terms of $\bar{\phi}$.

In preparation for the matching, we deduce from Eq. (15) the following inner representation of the outer representation of ϕ at the slot point k:

$$\phi = -\frac{q^{(k)}}{\pi} \ln r^{(k)} + \bar{\phi}(1,\theta^{(k)};x,t) + \sum_{i=1}^{N} q^{(i)} H^{(i,k)} + 0(r^{(k)}) \tag{17}$$

Here

$$H^{(i,k)} = -\frac{1}{\pi} \ln r^{(i,k)} - \frac{1}{\pi} \sum_{j=1}^{\nu} \frac{1}{j} \cos[j(\theta^{(k)} - \theta^{(i)})], \quad i \neq k$$

$$H^{(k,k)} = -\frac{1}{\pi} \sum_{j=1}^{\nu} \frac{1}{j} \qquad (i,k=1,\ldots,N) \tag{18}$$

with $r^{(i,k)}$ denoting the distance between the slot points i and k. The dominating part of the remainder corresponds to a tangential flow past the slot point.

VII. Inner Representations and Matching

The inner flows might be analyzed either in the transformed or the original cross-flow plane since the matching will involve only ϕ and the $q^{(i)}$, which all are invariant under the conformal mapping. We choose to work in the original plane, which clearly is the simplest alternative.

As explained in general terms in Sec. II, we shall work with a simplified slot flow model (Fig. 1) in which fast air from the test section enters the plenum chamber as a jet; in reverse flow, however, the fast air in the slot returns to the test section without separation, letting in quiescent air behind it to form a longitudinal separation bubble at plenum pressure $p_p^{(k)}$. Since the boundary S_p between the two masses of air is not precisely defined in the model, we can use this freedom to simplify the computation of the inner representation. More specifically, we shall assume, at least in the steady case, that for any given family of similar slot cross sections we can restrict ourselves to one basic cross-flow solution, taking the different positions of one of its material curves to represent possible free-boundary curves S_p. Then the slot flow model essentially is complete as soon as we prescribe the curve S_{po} at which the pressure condition is to be satisfied when there is a jet into the plenum chamber, and at which the jet is taken to split when the flow reverses. Introducing Cartesian coordinates (z,y) (Fig. 5), we take as the parameter for any curve S_p its intersection y_p with the y axis; y_{po}, the maximum value of y_p, corresponds to S_{po}.

Now let $a(x)$ be a measure of the width of the slot. The cross-flow velocity level in the slot and its neighborhood is given by $q^{(k)}/a$. In order for the relative position of S_p to be invariant in the limit $a \to 0$, we choose $q^{(k)} = 0(a^2)$, making the cross-flow velocity $0(a)$. The velocity set up by a streamwise variation of the slot width, as expressed by the

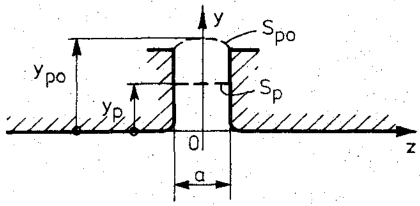

Fig. 5 Slot geometry.

normal velocity H in Eq. (3), should be compared with this. Being proportional to da/dx, it is evidently of the same order of magnitude. In addition to the sink-like flow into the slot corresponding to $q^{(k)}$, the geometry allows a cross flow essentially parallel to the wall. Its velocity is determined by the outer flow, and consequently is $0(q^{(k)})$. Therefore, we can neglect this flow component when writing down the inner representation of ϕ to the lowest order; to this order, a separation bubble remains aligned with the slot.

We first solve the sink-flow problem with $a=1$, $q^{(k)}=1$ and with vanishing deviation from the sink flow potential $-(1/\pi) \ln r^{(k)}$ for $y \to -\infty$. (How this can be done is demonstrated in an Appendix for the particular geometry of Fig. 5.) Let this normalized potential be $Q(z,y)$. This being the basic cross-flow solution out of which to construct S_p, it does not depend upon y_p. It is not valid beyond y_{po}, of course (see the Appendix). Then our inner representation is

$$\phi = \phi^{(k)} + q^{(k)} \cdot Q(z/a,\ y/a) + (da/dx) \cdot a \cdot A(z/a, y/a; y_p/a) \tag{19}$$

where A is a similarly normalized potential accounting for the effect of varying a. The unknown "constant" $\phi^{(k)}(x,t)$ is to be determined by matching to the outer flow.

Far away into the test section, Q and A have the representations

$$Q(z,y) = -\frac{1}{\pi} \ln r^{(k)} + 0\left(\frac{1}{r^{(k)}}\right) \quad A(z,y) = 0\left(\frac{1}{r^{(k)}}\right) \tag{20}$$

This implies that Q alone accounts for the net flux into the slot from the test section, whereas the flux of A, set up by the slot walls, all goes into the plenum chamber. The corresponding representation of ϕ is

$$\phi = \phi^{(k)} - \frac{q^{(k)}}{\pi} \ln\left(\frac{r^{(k)}}{a}\right) + 0\left(\frac{a}{r^{(k)}}\right)$$

and this can be matched to the outer representation (17). Hence,

$$\phi^{(k)} = \bar{\phi}(1,\theta^{(k)};x,t) + \sum_{i=1}^{N} q^{(i)} H^{(i,k)} - \frac{q^{(k)}}{\pi} \ln a \tag{21}$$

This important result permits us to relate $\bar{\phi}$ locally to the plenum pressures.

VIII. Plenum Pressure Condition in Steady Flow

So far the analysis applies in its main features to unsteady as well as steady flow. We now restrict ourselves to the steady case (to return later for a brief discussion of the unsteady case). In applying the pressure condition (5) we shall neglect the influence of varying slot width on the cross-sectional shapes of S_p and S_{po}. Consistent with this we shall satisfy the pressure condition only at $z=0$, $y=y_p$, or y_{po}. Furthermore, for A, which vanishes for $y_p \leq 0$, we shall use for $y_p > 0$ the one-dimensional approximation $A = -y^2/2$ $(0 \leq y \leq y_p)$. Hence, at $z=0$, $y=y_p$ (including $y_p = y_{po}$)

$$\phi_x + \frac{1}{2}\left[\frac{q^{(k)}}{a} v\left(\frac{y_p}{a}\right) - \frac{da}{dx}\frac{y_p}{a} E(y_p)\right]^2 = -\delta^{(k)}$$

$$(k=1,2,\ldots,N) \tag{22}$$

where $v(y)$ is the value of the y derivative of Q on $z=0$, and $E(y)$ is the unit step function. Similarly, in order to keep track of $y_p(x)$ when it is smaller than y_{po}, one has to solve the differential equation

$$\frac{\mathrm{d}y_p}{\mathrm{d}x}=\frac{q^{(k)}}{a}v\left(\frac{y_p}{a}\right)-\frac{\mathrm{d}a}{\mathrm{d}x}\frac{y_p}{a}E(y_p) \tag{23}$$

marching downstream from $x=x_o$, where $y_p=0$, and taking a new initial value y_{po} each time the jet splits on flow reversal.

Inserting ϕ from Eq. (19) into Eq. (22), with $\phi^{(k)}$ from Eq. (21), we obtain the pressure condition in the form

$$\frac{\mathrm{d}}{\mathrm{d}x}\Big\{\bar{\phi}(1,\theta^{(k)};x)+\sum_{i=1}^{N}q^{(i)}H^{(i,k)}$$
$$+q^{(k)}\left[Q\left(0,\frac{y_p}{a}\right)-\frac{1}{\pi}\ln a\right]-\frac{\mathrm{d}a}{\mathrm{d}x}\frac{y_p^{\,2}}{2a}E(y_p)\Big\}$$
$$+\frac{1}{2}\left[\frac{q^{(k)}}{a}v\left(\frac{y_p}{a}\right)-\frac{\mathrm{d}a}{\mathrm{d}x}\frac{y_p}{a}E(y_p)\right]^2=-\delta^{(k)} \tag{24}$$

If all of the fluxes $q^{(i)}(x)$ are known this is an ordinary differential equation for $\bar{\phi}(1,\theta^{(k)};x)$, which can be integrated together with Eq. (23), starting with a known value for $\bar{\phi}$ at the beginning of the slot.

IX. On Outer Boundary Conditions for Transonic Flows

At this stage, before we attempt to construct an outer boundary condition from the raw material gathered in the preceding sections, it might be useful to consider what sort of a boundary condition we should like to have. Now we are concerned with steady flows only, so that the differential equation with which to use the boundary condition is

$$\triangle\bar{\varphi}=[M^2-1+M^2(\gamma+1)\bar{\varphi}_x]\bar{\varphi}_{xx} \tag{25}$$

Typically, with those unbounded transonic flows for which the small-perturbation analysis is valid, the right-hand member is small as compared to the cross-flow derivatives, which constitute the left-hand member. We expect this to be true also in the present case, at least to the extent that we have been successful in designing a slotted test section with small interference. This means, of course, that the cross flow in any plane $x=$ const is approximately volume conserving, so that as much volume flux as is entering at the inner boundary (determined by the shape of the model), must leave through the outer boundary at about the same cross section. This constitutes a strong restriction on $\bar{\varphi}_n$ at the outer boundary in terms of $\bar{\varphi}_n$ at the inner boundary, suggesting that we might run into difficulties if we try to prescribe the normal derivative at the outer boundary.

These considerations come sharply into focus in the case of axisymmetric flow in the slender-body approximation, that is with the right-hand member of Eq. (25) neglected. Then the perturbation potential $\bar{\varphi}(x,r)$ takes the form

$$r\bar{\varphi}_r=s'(x) \qquad \bar{\varphi}=s'(x)\cdot\ln r+\bar{\varphi}(x,1)$$

where $s(x)$ is essentially the cross-sectional area of the body. In this case the radial velocity is everywhere exactly determined by the inner boundary condition, at the body, and only the potential itself can be prescribed at an outer boundary (at $r=1$, say). Therefore, we obtain a reasonable slender-body solution if the outer boundary is a jet boundary at prescribed pressure, or is a ventilated wall, which responds to the radial velocity $s'(x)$ with a well-defined pressure distribution. On the other hand, with a solid wall, at which zero normal derivative must be prescribed, there is no solution at all. Then the right-hand member must be retained in Eq. (25), accounting for the raised blockage interference level typical of choking.

Therefore we shall attempt to obtain our outer boundary condition in the form on

$$S_w\ :\ \bar{\varphi}=\mathfrak{F}[\bar{\varphi}_n] \tag{26}$$

where $\mathfrak{F}[\ ]$ is a regular functional over S_w (it becomes singular in the limit of a solid wall, of course). This choice carries with it the suggestion that, in solving Eq. (25) by an iterative numerical method, one should march back and forth between the model and the outer boundary, arriving each time at the outer boundary with an improved normal velocity to give, by Eq. (26), an improved pressure distribution to be carried back to the model. It is reassuring to note that employing such a scheme speeds up convergence, in particular in subsonic regions.[15] Our philosophy also suggests that the finite-difference approximation for the left-hand member of Eq. (25) should be a conservative one.

The choice of Eq. (26) should not, however, preclude interest in the inverse functional $\mathfrak{F}^{-1}$ giving $\bar{\varphi}_n$ in terms of $\bar{\varphi}$. Actually, if we are to adopt the idea of a self-correcting test section, presently being pursued in several laboratories, then a viable scheme might be to measure the wall pressure distribution along slats, essentially φ, and hence compute the normal velocity $\bar{\varphi}_n$ rather than trying to measure it.[12] For this $\mathfrak{F}^{-1}$ would be needed (together with a procedure for obtaining $\bar{\varphi}$ from φ; see Sec. XII). One would next have to compute the unbounded flow outside S_w, using $\bar{\varphi}_n$ in an inner boundary condition and obtaining an estimate of what $\bar{\varphi}$ should be on S_w in order to be free of interference. Using again the same $\bar{\varphi}_n$, one would then adjust the test parameters so as to make $\bar{\varphi}$, computed by Eq. (26) with the adjusted $\mathfrak{F}$, equal to $\bar{\varphi}$ obtained from the outer flow. Repeating this cycle as long as the required wall adjustments can be realized, employing $\mathfrak{F}^{-1}$ and $\mathfrak{F}$ alternately, one should end up with a slotted wall of minimum interference. Running the cycle backwards, adjusting $\bar{\varphi}_n$ for equality rather than $\bar{\varphi}$, would seem to be inviting difficulties.

X. Constructing the Outer Boundary Condition

According to the prescription of Sec. IV for the boundary condition on S_w, $\bar{\varphi}$ shall be related to $\bar{\varphi}_n$ in the same way as $\bar{\phi}$ is related to $\bar{\phi}_n$. To the extent that we have established this relationship, it is contained in Eqs. (16, 23, and 24).

We take Eq. (16) as a starting point, since it contains the normal derivative, the argument function of $\mathfrak{F}$. Substituting $\bar{\varphi}(x,r,\theta)$ for $\bar{\phi}(r,\theta;x)$, and specializing θ to the slot positions, we obtain

$$\sum_{i=1}^{N}\left\{\frac{1}{2}+\sum_{j=1}^{\nu}\cos[j(\theta^{(k)}-\theta^{(i)})]\right\}q^{(i)}$$
$$=\pi\cdot\bar{\varphi}_r(x,1,\theta^{(k)})\ (k=1,2,\ldots,N) \tag{27}$$

This is a linear system, which determines, for each x, the slot fluxes in terms of $\bar{\varphi}_r$. The coefficient matrix is independent of x and can be inverted numerically and stored as soon as the slot locations have been decided. Thus it is very simple to calculate the slot fluxes from $\bar{\varphi}_r$ (or from $\bar{\varphi}_n$ on an original noncircular S_w, for that matter). With uniformly distributed slots, the result is particularly simple: $q^{(k)}=(2\pi/N)\bar{\varphi}_r(x,1,\theta^{(k)})$.

Next we integrate Eqs. (23) to determine the flow penetration depth in the slots. This is straightforward, taking one slot at a time. Now the slot geometry is involved, however, so that the integration must be repeated each time we make a wall adjustment.

From Eq. (24), finally, we obtain the value of the potential at the slot positions:

$$\bar{\varphi}(x,1,\theta^{(k)}) = \varphi_o - [Q\left(0,\frac{y_p}{a}\right) - \frac{1}{\pi}\ln a]q^{(k)} + \frac{da}{dx}\frac{y_p}{a}E(y_p) - \sum_{i=1}^{N} H^{(i,k)}q^{(i)} - \int_{x_o}^{x}\left\{\frac{1}{2}\left[\frac{q^{(k)}}{a}v - \frac{da}{dx}\frac{y_p}{a}E(y_p)\right]^2 + \delta^{(k)}\right\}dx \quad (28)$$

satisfying, at $x=x_o$, the upstream condition for $\bar{\varphi}$ assumed in Sec. III. The right-hand member is now completely known. It would remain valid if we were to allow the plenum pressures to vary with x.

It is primarily Eq. (28) that we must analyze when we want to adjust slot flow parameters so as to produce the wall pressure distribution corresponding to interference-free flow. There will always be interference in the upstream part of the test section, for $x_o \le x \le x_1$ (Fig. 2). One should note here the singular behavior of $\bar{\varphi}$ at x_o, where not only a vanishes, but also $q^{(k)}$ (since Grad $\bar{\varphi}=0$ over the whole plane $x=x_o$). With the reasonable assumptions that $q^{(k)} \sim \frac{1}{2}q_{xx}^{(k)}\ \xi^2$ and $a \sim a_x\xi$ for $\xi = x-x_o \downarrow 0$, it follows from Eqs. (23) and (28) that

$$\bar{\varphi}_x(x_o+\xi,1,\theta^{(k)}) = -\delta^{(k)} + E(q_{xx}^{(k)})\frac{q_{xx}^{(k)}}{6a_x}v(0) + O(\xi\ln\xi)$$

For a smooth entrance flow, these limiting values of $\bar{\varphi}_x$ would have to agree with the constant value determined by M_o, and this requirement would determine the plenum pressures. It might not be important that the flow at x_o is smooth, however. It would, for example, seem more important to establish the required flow smoothly over the plane $x=x_1$, downstream of which we want to eliminate the wall interference. The first claim to setting the plenum pressures right, as well as the entrance Mach number, goes of course to those parts of the walls which might influence the flow at the model most strongly.[16]

In order to complete the construction of the functional $\mathfrak{F}$, we have only to define $\bar{\varphi}$ between slots. In accordance with our method of analysis this is done, in each plane $x=$const, by trigonometric interpolation of order ν. Obviously ν must be chosen so as to make $2\nu+1$ equal to N at most; usually it will be smaller. This means that usually we cannot satisfy the conditions of Eq. (28) precisely. A least-squares fit then could be used, which again calls for storing a precomputed constant matrix. The deviations, of course, correspond to higher-order components to be filtered out. Since both Eqs. (23) and (28) are nonlinear with respect to $q^{(i)}$, such components will arise even if not present in the $\bar{\varphi}_r$ used in Eq. (27).

The inverse functional is not so easily constructed, because of the nonlinearity of the equations from which the fluxes $q^{(i)}$ corresponding to a given potential on S_w are determined. An iterative scheme must be set up. Once the fluxes are known, the normal derivative is immediately obtained from Eq. (27) at the slot positions. The construction again is completed by trigonometric interpolation.

XI. Symmetric Flow

As a simple application, consider the case of an axisymmetric body along the axis of a circular test section with N uniformly distributed identical slots ($N>1$). From symmetry, the flow is periodic with respect to θ with period $2\pi/N$. The potential φ therefore will be independent of θ to order $N-1$ in a trigonometric expansion. Since $N-1$ is larger than $(N-1)/2$, the greatest value for ν, we conclude that $\bar{\varphi}$ is independent of θ. Actually, since the flux through each slot is given by

$$q = d\cdot\bar{\varphi}_r(x,1) \qquad d=2\pi/N(=\text{arc between slots}) \quad (29)$$

and is independent of ν, we will get the same $\bar{\varphi}(x,r)$ for all permitted values of ν.

Equation (29) takes the place of Eq. (27). It remains to consider Eqs. (23) and (28). Noting that, in the present case,

$$\sum_{i=1}^{N} H^{(i,k)} = -\frac{1}{\pi}\ln N$$

we obtain, in the case of constant slot width,

$$\frac{dy_p}{dx} = v\left(\frac{y_p}{a}\right)\frac{d}{a}\bar{\varphi}_r(x,1) \quad (30)$$

and

$$\bar{\varphi}(x,1) = \varphi_0 - K\bar{\varphi}_r(x,1) - \int_{x_o}^{x}\left[\frac{1}{2}(v\frac{d}{a}\bar{\varphi}_r)^2 + \delta\right]dx \quad (31)$$

with

$$K = d\left[\frac{1}{\pi}\ln\frac{2d}{\pi a} - \frac{1}{\pi}\ln 4 + Q(0,y_p/a)\right] \quad (32)$$

Equation (31) agrees with the classical formula, augmented by a quadratic cross-flow term in the manner of Wood.[17] It is shown in the Appendix that Eq. (32) is a second-order approximation for small a/d to the classical, as well as the generalized[4], K.

It may seem remarkable that $\bar{\varphi}$ is independent of θ. It does not mean, however, that the wall interference is totally independent of the number of slots, not even for a fixed $\bar{\varphi}$. In adding slots we suppress successively higher harmonics, which were neglected in $\bar{\varphi}$ (but present in φ) when the slots were fewer. We obtain, from Eq. (15), the simple expression

$$\varphi - \bar{\varphi} = -(2/N)\bar{\varphi}_r\cdot\ln(1-r^N)$$

for the θ-dependent part of the interference along the radius to a slot point (in the outer approximation). It is clearly seen (Fig. 6) how, with increasing number of slots, the central region of constant interference grows (compare Fig. 5 of Ref. 7). Already eight slots make approximately two-thirds of the test section width available for interference-free flow (the conclusion might be different for nonsymmetric flows, of course).

The outer boundary condition $\bar{\varphi} = \mathfrak{F}[\bar{\varphi}_r]$, as constituted by Eqs. (30-32), has been tested quite extensively[4] with the numerical method of Ref. 15. No difficulties were found, except where the slot width was very small (smaller than that normally used), in which case the convergence became slow. This is not surprising of course, since $\mathfrak{F}$ is singular in the limit of a solid wall.

XII. Analysis of Wall Pressures

For a further application, assume that we want to determine $\bar{\varphi}$ on S_w by measuring the pressure distribution along slats, say, at constant $\theta=\theta_w \neq \theta^{(i)}$. We first integrate Eq. (4) along the slat to get φ (the quadratic cross-flow term can be neglected in this case). Then, from Eqs. (7) and (15), we have

$$\bar{\varphi} = \varphi + \bar{\phi} - \phi = \varphi + \frac{1}{\pi}\sum_{i=1}^{N} q^{(i)}\left\{\ln r_w^{(i)} + \sum_{j=1}^{\nu}\frac{1}{j}\cos[j(\theta_w - \theta^{(i)})]\right\} \quad (33)$$

where $r_w^{(i)}$ is the cross-flow distance from a pressure tap to the slot point i. In the case of symmetric flow, with θ_w half way between slots, this reduces to

$$\bar{\varphi} = \varphi + (d\cdot\ln 2/\pi)\cdot\bar{\varphi}_r \quad (34)$$

in agreement with Ref. 4.

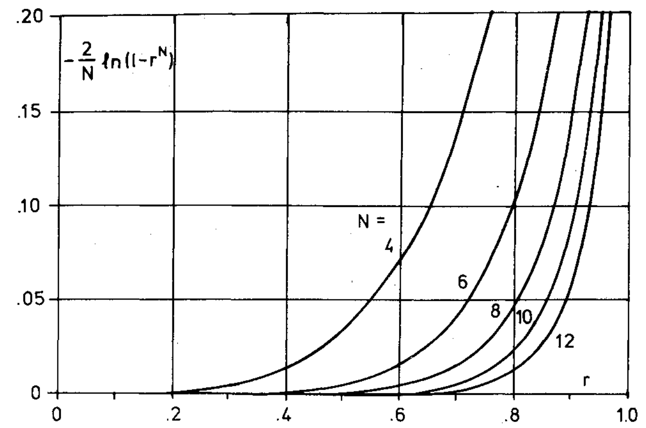

Fig. 6 Symmetric flow: variation of interference along the radius to a slot (to be compared with K, which typically has the value 0.6).

The application of Eq. (33) is straightforward if we know the fluxes; however, they are not known in the interesting case when we want to determine $q^{(i)}$ and $\bar{\varphi}_r$ by applying $\mathfrak{F}^{-1}$ to $\bar{\varphi}$. However, $\bar{\phi}-\phi$ has the character of a small correction, so that there is little doubt that an iterative scheme, using successively improved estimates for $q^{(i)}$, will converge rapidly. This is not really very much of a complication; $\mathfrak{F}^{-1}$ must be computed iteratively anyway.

XIII. Unsteady Flow

In the first seven sections, the analysis applies, in its main features, also to unsteady flows. In the pressure condition (5), however, we must add φ_t/U to φ_x, recognizing at the same time that the free surface S_p might move, and that the plenum pressures $\delta^{(i)}$ are no longer known in advance, since pressure waves may propagate into the plenum chamber. The simplified picture of the slot flow introduced in Sec. VII should be extended to include a potential which describes the cross-flow due to the motion of S_p, in addition to the potential Q, which describes the cross-flow due to the obliqueness of the flow. (This approach means, of course, that we are assuming the slot width to be small as compared to typical wavelengths of the unsteady flow.) The additional cross-flow is somewhat different in that it involves the quiescent air of the plenum chamber, as well as the fast air in the slot. This also will add a new contribution to the right-hand member of Eq. (23) for S_p, the left-hand member of which now goes over into $[\partial/\partial x+(1/U)\partial/\partial t]y_p$, of course. All of these effects combine to make the pressure condition corresponding to Eq. (24) rather complicated in its final form.

In order to account for fluctuations in $\delta^{(i)}$, we must analyze the wave propagation in the plenum chamber, a forbidding task. The simplest case arises if the plenum chamber is so large that only waves propagating from the slots into the plenum chamber contribute to the pressure fluctuation on $S_{po}+S_p$. These waves correspond to the additional, nonsteady part of the slot flow, and so can be analyzed, assuming a known steady pressure deeper inside the plenum chamber. In the next more complicated case, one would have to account for varying plenum pressure in the manner of the classical Helmholtz resonance analysis. It seems that in these two cases there is a reasonable chance to complete the analysis and construct a homogeneous boundary condition for the test section flow. Perhaps it will be necessary to linearize the problem, assuming the unsteadiness to be a small perturbation of a steady flow.

XIV. Wall Interference Corrections Test Section Calibration

Suppose we have succeeded in adjusting the test parameters so as to make the interference negligible at the model. Then three wall corrections of classical type are immediately available from this process: a Mach number correction ($=M-M_o$), an angle-of-attack correction (= the angle of attack of the test section with respect to the direction of the unbounded flow simulated), and an angle-of-yaw correction (= the corresponding angle of yaw of the test section).

The other classical corrections, those for induced buoyancy and flow curvature, are rightly absent. As soon as they are needed there is a distortion of the pressure distribution over the model that cannot be tolerated. In contrast, the former corrections are not associated with any such distortion and should be permitted to be large if it helps in reducing the interference. This is "the principle of minimizing interference rather than corrections,"[18] implying the concept of a "correctable-interference transonic wind tunnel."[19]

There might be other errors present in the test section flow; errors that are not accounted for when computing the wall interference. Disturbances from the entrance section upstream of the slots, axial gradients set up by the wall boundary layers or by improper alignment of the walls, or upstream influence from the model support system are examples. The main tool for handling such errors is calibration, running the test section empty with the walls and plenum pressures set for uniform flow or some other well-defined flow. Such errors should be eliminated by proper adjustment of the test section and slots, not by introducing corrections to the test data. The practice of using the Mach number of the empty test section, calibrated against the plenum pressure, as a freestream reference Mach number for model tests does not seem to make sense in the context of the present theory.

XV. Concluding Remarks

The present inviscid theory of wall interference in slotted test sections generalizes to three-dimensions the theory for two-dimensional tests, developed on a classical basis[5,17] in Ref. 4. In analyzing the local flow at each slot separately, the structure of the theory facilitates later inclusion of corrections to account for viscous effects inside the slots and the plenum chamber. A first attempt in this direction has been made already,[4] and as more extensive comparisons with experiment are completed, it might become possible to extend and delineate the area in which the inviscid theory, with or without corrections, might be used with confidence. The interaction of shock waves with the slot flow must be studied, in particular.

Meanwhile, the inviscid theory can be used for running numerical experiments. These will show how accurately one must describe the action of the slotted wall in different types of application, and what wall adjustment facilities one must provide in order to eliminate the wall interference. They also will help in developing strategies for efficient use of adaptive slotted walls in future wind tunnels.

Appendix: Simplified Analysis of Slot Flow

As a basis for analyzing the slot flow for the geometry of Fig. 5, consider the symmetrical flow of unit flux from a half-plane into a slot of unit width and unlimited depth (Fig. A1). We shall determine the velocity potential $Q(z,y)$, normalized to have vanishing deviation from the sink flow potential $-(1/\pi)\ln r^{(k)}$ for $y\to-\infty$. This is accomplished by mapping the flow region conformally onto a half-plane ($-\pi\leq\vartheta\leq 0$ in Fig. A2), transforming the slot extremity ($Z=i\infty$) into the origin and leaving the far-field undisturbed. The required complex transformation is

$$Z=z+iy=e^{i\vartheta}\sqrt{s^2-\sigma^2e^{-2i\vartheta}}-i\sigma\ln\frac{\sqrt{s^2-\sigma^2e^{-2i\vartheta}}+i\sigma e^{-i\vartheta}}{s}$$

$$\sigma=\frac{1}{\pi} \tag{A1}$$

where (s,ϑ) are polar coordinates in the transformed plane ζ.

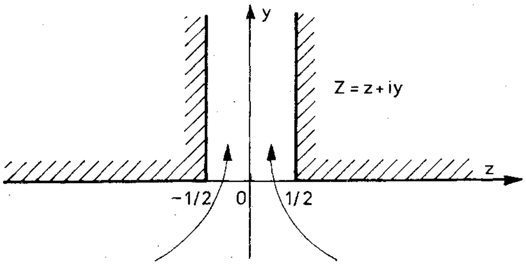

Fig. A1. Basic slot flow.

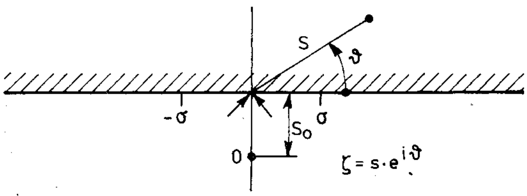

Fig. A2. Transformed slot flow.

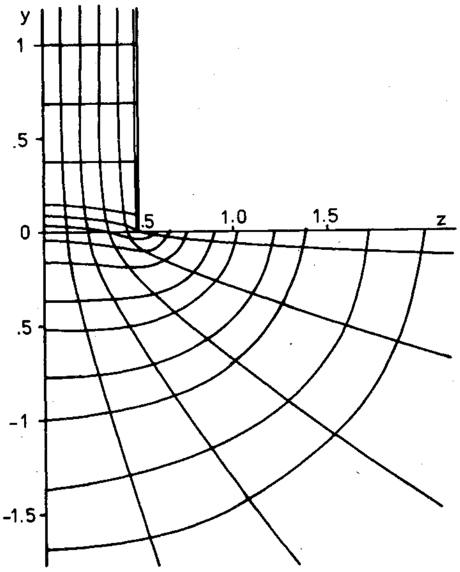

Fig. A3. Positions of material curve taken to describe possible cross sections of the free surface S_p (the streamlines are also shown).

The exterior wall and the slot walls are mapped onto the real axis with the corner points at $\pm\sigma = \pm 1/\pi$. The flow is that of a sink at the origin with potential

$$Q = -(1/\pi)\ln s \tag{A2}$$

We choose as the material curve representing, in its different positions, possible free-boundary curves S_p, one that is a straight line across the slot, far into the slot. In the transformed plane the curve, when close to the origin, is a circle. In order to determine its development, we can integrate along streamlines (rays) in the transformed plane. Points on the same curve must have the same value of the parameter

$$t(s,\vartheta) = \int_\epsilon^s \left|\frac{dZ}{d\zeta}\right|^2 s\, ds \tag{A3}$$

where ϵ is a small positive number. After the curves have been determined in the ζ plane, they have to be transformed back into the Z plane. The result is depicted in Fig. A3.

For our immediate purpose, it is sufficient to consider the intersection y_p of S_p with the axis of symmetry. This is mapped on the negative imaginary axis. The value of s

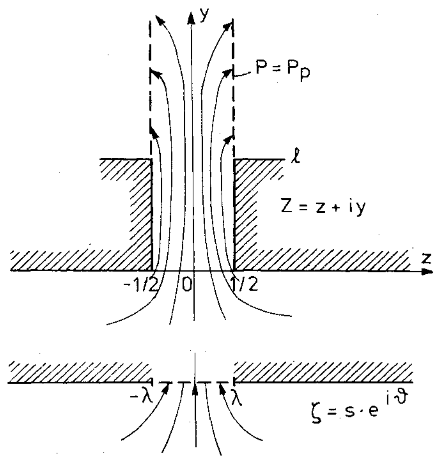

Fig. A4. Slot flow with a jet.

corresponding to y on $z=0$ is obtained from the equation

$$\sqrt{s^2+\sigma^2}+\sigma\,\ln\frac{\sqrt{s^2+\sigma^2}-\sigma}{s} = -y \tag{A4}$$

Once $s(y)$ is known, it is straightforward to compute Q and v:

$$Q(0,y) = -\frac{1}{\pi}\ln s \qquad v = \frac{1}{\sqrt{1+(s/\sigma)^2}} \tag{A5}$$

If y is well inside the slot, we can take s/σ to be small. Expanding the square root in Eq. (A4), the following second-order approximation is obtained:

$$-\ln s = 1-\ln(2/\pi)+\pi y+e^{-2(\pi y+1)} \tag{A6}$$

Hence

$$Q(0,y) = \frac{1}{\pi}\left(1-\ln\frac{2}{\pi}\right)+y+\frac{1}{\pi}e^{-2(\pi y+1)}$$

$$v(y) = 1-2e^{-2(\pi y+1)} \tag{A7}$$

Inserting into Eq. (32), we obtain

$$K = d\left[\frac{1}{\pi}\ln\frac{2d}{\pi a}+\frac{1}{\pi}\left(1-\ln\frac{8}{\pi}\right)+\frac{y_p}{a}+\frac{1}{\pi}e^{-2(\pi y_p/a+1)}\right] \tag{A8}$$

in complete agreement (to second order in a/d) with the result of Ref. 4, at least for $y_p/a > 0.1$.

This result is valid if S_p is inside the slot. If the flow is leaving the slot as a jet into the plenum chamber, the situation is more complicated, since the width of the jet might vary with x. This means that Q is no longer sufficient for describing the cross-flow due to $q^{(k)}$ in Eq. (19), but that a new additional term is needed, say one corresponding to a flow where the whole flux goes into widening the jet. It follows from the y invariance of the pressure condition (5), if the influence of varying flow type on the nonlinear term can be neglected, that the additional flow is one of constant potential on the jet boundary. This leads to a new normalized cross-flow potential $P(z,y)$, which is similar to $Q(z,y)$ in the upstream region (Fig. A4), but satisfies the condition $p = \text{const}\ (= P_p)$ on $z = \pm 1/2$ for $y > \ell > 0$ (ℓ = slot depth). If the points $z = \pm 1/2$, $y = \ell$ are mapped onto $s = \lambda$, $\vartheta = 0$, and $-\pi$, then, in the transformed plane, we obtain immediately

$$P = -\frac{1}{\pi}\ln\left|\frac{1}{2}s\,e^{i\vartheta}\left[1+\sqrt{1-\left(\frac{\lambda}{s e^{i\vartheta}}\right)^2}\right]\right|$$

Hence, on the jet boundary,

$$P_p = \frac{1}{\pi} \ln \frac{2}{\lambda} = Q + \frac{1}{\pi} \ln \frac{2s}{\lambda}$$

This means that the two potentials, which in the region upstream of the jet are closely equal, again become equal a short distance downstream of the slot, at $s = \lambda/2$. This is where we put our boundary S_{po} across the jet. Then we do not have to determine how much of the cross-flow is of the Q type, and how much is of the P type. We compute as if it is all of the Q type, and satisfy the plenum pressure condition on the y axis at

$$y_{po} = \ell + (\ln 2/\pi) a (1 + 2e^{-2(\pi\ell/a+1)}) \quad \text{(A9)}$$

which is the approximation corresponding to Eq. (A6). This agrees with the value obtained in Ref. 4.

When there is a bubble, for $y_p < 0$, Eq. (A4) again can be solved approximately. The result, for $s \gg \sigma$, is

$$s = -y\left(1 + \frac{5}{8\pi^2} \frac{1}{y^2}\right) \quad \text{(A10)}$$

hence

$$Q(0,y) = \frac{1}{\pi} \ln y - \frac{5}{8\pi^2} \frac{1}{y^2}, \qquad v = \frac{1}{\pi} \frac{1}{y}\left(1 - \frac{5}{4\pi^2} \frac{1}{y^2}\right) \quad \text{(A11)}$$

The corresponding result for K is

$$K = d\left[\frac{1}{\pi} \ln \frac{d}{2\pi |y_p|} - \frac{5}{8\pi^3} \frac{1}{(y_p/a)^2}\right] \quad \text{(A12)}$$

Finally, it might be noted that the preceding analysis, with very minor modifications, applies also to a slot located in a right-angled corner. One has only to make the axis of symmetry into a wall, and everything else follows.

Acknowledgments

This is an updated version of the ICAS paper 76-03 presented at the 10th ICAS Congress in Ottawa, Canada, Oct. 4-8, 1976. The research reported herein was sponsored jointly by the FFA and the U.S. Air Force Office of Scientific Research under Grant No. AFOSR 72-2184.

References

[1] Wright, R. H., "The Effectiveness of the Transonic Wind-Tunnel as a Device for Minimizing Tunnel-Boundary Interference for Model Tests at Transonic Speeds," AGARD Rept. 294, 1959.

[2] Goethert, B. H., *Transonic Wind Tunnel Testing*, edited by. W. C. Nelson, AGARDograph 49, Pergamon Press, 1961.

[3] Berndt, S. B., "Theory of Wall Interference in Transonic Wind Tunnels," *Symposium Transsonicum 1962*, edited by K. Oswatitsch, Springer-Verlag, 1964, pp. 288-309.

[4] Berndt, S. B. and Sörensén, H., "Flow Properties of Slotted Walls for Transonic Test Sections," AGARD Conference Proceedings, No. 174, Paper No. 17, 1975.

[5] Guderley, G., "Simplifications of the Boundary Conditions at a Wind-Tunnel Wall with Longitudinal Slots," Wright Air Development Center, TR 53-150, 1953.

[6] Baldwin, Jr., B. S., Turner, J. B., and Knechtel, E. D., "Wall Interference in Wind Tunnels with Slotted and Porous Boundaries at Subsonic Speeds," NACA TN 3176, 1954.

[7] Davis, D. D. and Moore, D., "Analytical Studies of Blockage- and Lift-Interference Corrections for Slotted Tunnels Obtained by the Substitution of an Equivalent Homogeneous Boundary for the Discrete Slots," NACA RM-L53E07b, 1953.

[8] Maeder, P. F., "Theoretical Investigation of Subsonic Wall Interference in Rectangular Slotted Test Sections," Brown University, Division of Engineering, TR WT-11, 1953,

[9] Woods, L. C., *The Theory of Subsonic Plane Flow*, Cambridge University Press, Cambridge, 1961.

[10] Barnwell, R. W., "Improvements in Slotted-Wall Boundary Condition," *Proceedings of the AIAA 9th Aerodynamic Testing Conference*, 1976, pp. 21-30.

[11] Garner, H. C., et al., "The Theory of Interference Effects on Dynamic Measurements in Slotted-Wall Tunnels at Subsonic Speeds and Comparison with Experiment," Aeronautical Research Council, R&M 3500, 1966.

[12] Ferri, A. and Baronti, P., "A Method for Transonic Wind-Tunnel Corrections," *AIAA Journal*, Vol. 11, Jan. 1973, pp. 63-66.

[13] Baronti, B., Ferri, A., and Weeks, Th., "Analysis of Wall Modification in a Transonic Wind Tunnel," Advanced Technology Laboratories, Inc., Rept. ATL TR 181, 1973.

[14] Tuck, E. O., "Matching Problems Involving Flow through Small Holes," *Advances in Applied Mechanics*, Vol. 15, 1975, pp. 90-158.

[15] Sedin, Y. C.-J., "Axisymmetric Sonic Flow Computed by a Numerical Method Applied to Slender Bodies," *AIAA Journal*, Vol. 13, April 1975, pp. 504-511.

[16] Berndt, S. B., "Theoretical Aspects of the Calibration of Transonic Test Sections," *Zeitschrift für Angewandte Mathematik und Physik*, Vol. IXb, 1958, pp. 105-124.

[17] Wood, W. W., "Tunnel Interference from Slotted Walls," *Quarterly Journal of Mechanics and Applied Mathematics*, Vol. 17, May 1964, pp. 126-140.

[18] Berndt, S. B., "On the Influence of Wall Boundary Layers in Closed Transonic Test Sections," FFA Rept. 71, 1957.

[19] Kemp, W. B., Jr., "Toward the Correctable-Interference Transonic Wind Tunnel," *Proceedings of the AIAA 9th Aerodynamic Testing Conference*, 1976, pp. 31-38.